Exp Brain Res (2003) 152:317–322
DOI 10.1007/s00221-003-1530-5

RESEARCH ARTICLE

Ian M. Purcell · Shawn D. Newlands · Adrian A. Perachio

Responses of gerbil utricular afferents to translational motion

Received: 12 August 2002 / Accepted: 1 May 2003 / Published online: 31 July 2003

Abstract In the present study, we report the sensitivity of utricular afferents to sinusoidal translational motion in the horizontal plane. The head orientation was altered relative to the direction of translational travel in 30° increments to allow determination of the head orientation that elicited the maximal and minimal responses of each afferent neuron. We determined gain and phase relationships at a constant peak linear acceleration of 0.1 g applied at frequencies between 0.20 and 2.0 Hz for multiple head orientations. The response dynamics and vector of maximal sensitivity for the utricular afferents are consistent with those reported for other mammalian species. Irregularly (CV>0.3) and intermediate ($0.1 \leq CV \leq 0.3$) discharging units demonstrated gain enhancement at higher frequencies. Regular units (CV<0.1) showed lower gains and flat response dynamics. The mean gains of the irregular, intermediate, and regular units at 0.5 Hz were 256, 118, and 69 spikes s^{-1} g^{-1}, respectively. The phase of the response was independent of the vector of orientation except near the null response orientation where phase and gain were difficult to accurately measure. Phase leads (relative to acceleration) in irregular units at lower frequencies were reduced at higher frequencies. All afferents demonstrated simple one-dimensional tuning with their vectors of maximal sensitivity distributed throughout the 360° of the horizontal plane, though the majority were directed out of the contralateral ear.

Keywords Vestibular nerve · Utricle · Vestibular afferents · Gerbil · Response dynamics

S. D. Newlands · A. A. Perachio (✉)
Department of Otolaryngology,
University of Texas Medical Branch,
301 University Boulevard, 7.102 Medical Research Building,
Galveston, TX 77555–1063, USA
e-mail: aperachi@utmb.edu
Tel.: +1-409-7722721
Fax: +1-409-7725893

I. M. Purcell
Department of Neurology, UCSD Medical Center,
200 West Arbor Drive, San Diego, CA 92103–8465, USA

A. A. Perachio
Departments of Anatomy & Neurosciences,
and Physiology & Biophysics,
University of Texas Medical Branch,
Galveston, TX 77555, USA

Introduction

Sensory information related to gravity and head movement as we move through space is encoded and processed by the vestibular system to modulate and control postural and oculomotor reflexes and spatial orientation. Semicircular canal and otolith related organs within the vestibular labyrinth contain sensory neuroepithelia with hair cells sensitive to angular and linear accelerations, respectively. The sensory neuroepithelia of the bilateral otolith (utricular and saccular) maculae convey information about head position relative to gravity and translational acceleration as excitatory input to the vestibular afferent neurons. The peripheral terminal fields of the afferent neurons originate in relatively discrete areas of the utricular macula (Fernández et al. 1990; Baird and Schuff 1994; Si et al. 2003) and the response of an individual afferent neuron is determined by the sensitivity to deflection of hair cells in its peripheral terminal field (Goldberg et al. 1990). The response characteristics of utricular afferents have been described in a number of species and stereotypically vary with discharge regularity (Fernández et al. 1972; Fernández and Goldberg 1976b; Perachio and Correia 1983; Goldberg et al. 1990; Si et al. 1997; Angelaki and Dickman 2000). Studies in chinchillas and squirrel monkeys show that regularly firing otolith afferents display response gains that are almost constant and response phases that are near peak head acceleration over tested frequencies. More irregularly firing afferents display increasing response gains (5 to 20-fold) and response phase leads as frequency is increased (Fernández and Goldberg 1976b; Goldberg et al. 1990).

The present study was conducted to document the response dynamics of gerbil utricular afferents to pure

linear translation. Single unit recordings of gerbil utricular afferents during translational motion on a horizontal sled were examined at frequencies between 0.20 and 2.0 Hz. Comparison can thus be made between this rodent species and the only other published data for studies utilizing pure translational stimuli from experiments conducted on rhesus monkeys (Angelaki and Dickman 2000) and pigeons (Si et al. 1997). Comparisons can also be made to response dynamics to eccentric rotation stimuli reported from experiments done in squirrel monkeys (Fernández and Goldberg 1976b) and chinchillas (Goldberg et al. 1990).

Materials and methods

Surgical procedures

Forty gerbils (*Meriones unguiculatus*) of both sexes and weighing from 70 to 100 g were used in the present study. All procedures were performed according to the National Institutes of Health *Guide for the Care and Use of Animals in Research* and were reviewed and approved by the University of Texas Medical Branch's Institutional Animal Care and Utilization Committee. All surgery was performed under aseptic conditions with general anesthesia. Gerbils were initially anesthetized with an intraperitoneal injection of pentobarbital sodium (25 mg/kg) followed within 5 min by an intramuscular injection of ketamine (25 mg/kg). Supplementary doses of ketamine were administered as needed to maintain anesthesia. Core body temperature as measured by a thermistor rectal probe was maintained in a range of 36.5–38°C by a sodium acetate-heating pad. The animals were then placed in a stereotaxic frame and the head mounted with the nose tilted down 20° with respect to the interaural axis to align the major plane of the utricular maculae and horizontal semicircular canals coplanar with the earth horizontal plane during subsequent stimulation protocols. This will be referred to hereafter as the standard head position. A midline scalp incision was performed and a 0.6-mm dental burr used to make a 2 × 2 mm hole in the dorsal calvaria, exposing the dorsal surface of the cerebellum.

Stimulation protocols

The animal and stereotaxic frame were mounted on gimbals allowing yaw and pitch rotation. The pitch axis was the interaural axis of the head. The yaw axis was aligned with the orientation of the earth gravitational vector and intersected the interaural axis at its center. The gimbals were secured to a plate that was attached to a completely captured air-bearing sled driven along a 10-ft slab of optically polished granite with 8 ft of usable travel. The bearings supported the load above the granite slab. A 40 ft-lb servo-controlled DC torque motor was coupled to the sled via a cable wound about a capstan directly attached to the motor drive shaft, and linear acceleration stimuli were generated by controlled translational motion of a sled bearing the preparation. An analog function generator provided control signals for the stimuli that consisted of single harmonic translational sinusoids in the horizontal head plane ranging in frequency from 0.20 to 2.0 Hz at a constant peak acceleration of ±0.1 g. Sled position was measured continuously through a precision potentiometer mounted directly onto the drive shaft of the motor, and acceleration was verified by X, Y, and Z axis linear accelerometers bolted near the animal's head on the stereotaxic unit.

Linear acceleration stimuli coplanar to the earth horizontal plane were defined according to a coordinate system in which a vector of positive linear acceleration directed out the nose of the animal is assigned a vector angle of 0° (Angelaki et al. 1993). We then operationally defined a vector of positive linear acceleration directed out the left ear as 90° and out the right ear as 270°.

The test protocol consisted of translational sinusoids at different vector orientations of the animal's head. Orientations of the head with respect to the direction of travel were indexed every 30° through 180° to 360°. For most neurons, the stimulus parameter first tested was 0.5 Hz, ±0.1 g. After recording responses at multiple vector polar angles at that frequency, we attempted to inject some of the neurons intra-axonally with horseradish peroxidase. Results from these injections are not reported here. For some units, data were collected at 0.20, 0.25, 1.0, 1.5, and/or 2.0 Hz. At least six cycles of responses were collected at 0.20 or 0.25 Hz, eight cycles at 0.5 Hz, 15 cycles at 1.0 Hz, and 20 cycles at 2.0 Hz.

Unit recordings

A stereotaxic electrode carrier bearing a microdrive was positioned at an angle of 25° off the sagittal head plane to direct horseradish peroxidase (10%) or saline (2 M) filled micropipettes (40–60 MOhms @135 Hz) to the vestibular nerve. The electrode was advanced through the cerebellum and brainstem into the vestibular nerve using the microdrive. Single unit recordings were made from afferents in the post-ganglionic portion of the vestibular nerve. Fibers with horizontal translation sensitivity and no response to horizontal rotational motion in the yaw plane were assumed to be otolith organ related. There was concern about horizontal responses from saccular afferents in the horizontal plane, though most saccular hair cells have morphophysiological orientations that are not in the horizontal plane (Lindeman 1969; Curthoys et al. 1999). Operationally, afferents with vectors of maximal sensitivity directed out the nose (0°) or tail (180°) that demonstrated a rapid gain roll-off (within 15°) as the animal is repositioned away from the naso-occipital axis, and thus away from the major plane of the saccule, were thought to be saccular related. Such afferents were easily identified and excluded from the analysis. Other evidence for the utricular origin of the recorded afferents was close association with lateral and anterior canal afferents. Posterior canal afferents were not recorded in close proximity to presumed utricular afferents. In contrast, posterior canal afferents were recorded near presumed saccular afferents, suggesting that the electrode was in the posterior division of the vestibular nerve. Once a unit was classified as utricular related, the recording protocol included collection of unit activity while the head was motionless and oriented in the standard head position. Dynamic responses to translational motion were tested for each unit as described above. Neural activity was amplified (x1000), bandpass filtered (100 to 10 KHz), displayed on an oscilloscope, sent to an audio monitor, and stored on VHS tape. The position signal was recorded on the tape as well.

Data analysis

Data were analyzed off-line as described previously (Angelaki et al. 1993). In brief, the taped unit signal was played back through a time/amplitude window discriminator to convert each unit into a timed spike. Firing rate cycle histograms were computed (256 bins per cycle for each stimulus frequency). The cycle histogram for the response and the digitized stimulus waveform sampled at 100 Hz were independently subjected to a linear curve-fitting routine to compute the least-squares fit of the sum of two sinusoids representing the first and second harmonics of the stimulus. Gains were expressed as the ratio of peak firing frequency to peak stimulus intensity (in spike s^{-1} g^{-1}) for the first harmonic frequency, which usually accounted for 95% or greater of the response. The phase of the fundamental component of the response was expressed as the difference in degrees between peak fitted averaged firing frequency and peak fitted linear acceleration. Both gain and phase are expressed with regard to linear acceleration, and phase leads are represented by positive values.

The gain of presumed utricular units was obtained for translation in the different head orientations. The gains were calculated such that the phase relationship between the stimulus and response, with regard to acceleration, is within ±90° by inverting the sign of the gain for responses with phase relationships of 90° to 270° with

respect to the stimulus. For example, a gain of 100 spikes s^{-1} g^{-1} with a phase relationship of 170° was plotted as a gain of –100 spikes s^{-1} g^{-1} (phase –10°). The gain was then plotted vs. orientation. The response gains varied as a sine function relative to their responses to their maximum sensitivity vector. The maximum response gain values (gmax) were interpolated as the peak of the sine function. The maximum sensitivity vectors (Smax) is the interpolated orientation of linear acceleration that results in gmax. This method is mathematically identical to a rectified cosine fit (Fernández et al. 1972; Loe et al. 1973; Blanks et al. 1975; Fernández and Goldberg 1976a).

Results

Eighty-five cells in the right and left utricular nerves were isolated and recorded for sufficient duration to determine the two-dimensional maximum sensitivity vector and response characteristics of the units at one frequency. Analysis of one neuron is shown in Fig. 1. The curve fits of the response to the vectors oriented closest to peak and closest to null are shown in Fig. 1A, B. A response plot of gain as a function of head orientation is shown in Fig. 1C. As a measure of background discharge, activity was recorded in 79 of the 85 cells while the head was statically held in the standard position. In 10 cells the dynamics were characterized at two frequencies, in 1 cell at three frequencies, in 9 at four frequencies, and in 5 at five frequencies. In the 60 cells recorded with full characterization of response vectors at only one frequency, recording of the cell's dynamic responses was cut short due to attempts to intracellularly label the cell.

Off-line analysis of the average spontaneous firing activity and the variability of discharge rate was performed on each neuron in the standard test position. The mean interspike interval (ISI), discharge rate (spikes s^{-1}), and coefficient of variation (CV= SD/mean) of the ISI's were calculated. The CV was used as a measure of regularity of neuronal firing. Due to the natural separation of the calculated CV's, we operationally divided the data into a group of highly regular firing neurons with CV's less than 0.1, a group of intermediate firing neurons with CV's ranging from 0.1 to 0.3, and a group of highly irregular firing neurons with CV's greater than 0.3. The distribution of CV's is shown in Fig. 2A, and the relationship between CV and ISI is shown in Fig. 2B. The average discharge rate for all 79 units was 53.1±31.1 (mean±SD) spikes s^{-1}. Twenty-two of the units classified as regularly firing had a mean resting discharge rate of 64.1±18.9 (mean±SD) spikes s^{-1}, 13 classified as intermediately firing had a mean discharge rate of 51.1±24.9 (mean±SD) spikes s^{-1} and 44 classified as irregularly firing had a mean discharge rate of 48.2±36.3 (mean±SD) spikes s^{-1}. There was not a significant difference between the mean discharge rates for these three classes of neurons (ANOVA, $P>0.05$).

The gain and maximum sensitivity vector relationships of the recorded utricular afferent neurons were examined. At a given frequency, the gain of a unit varied with head position as a rectified cosine function (Fig. 1C). The head

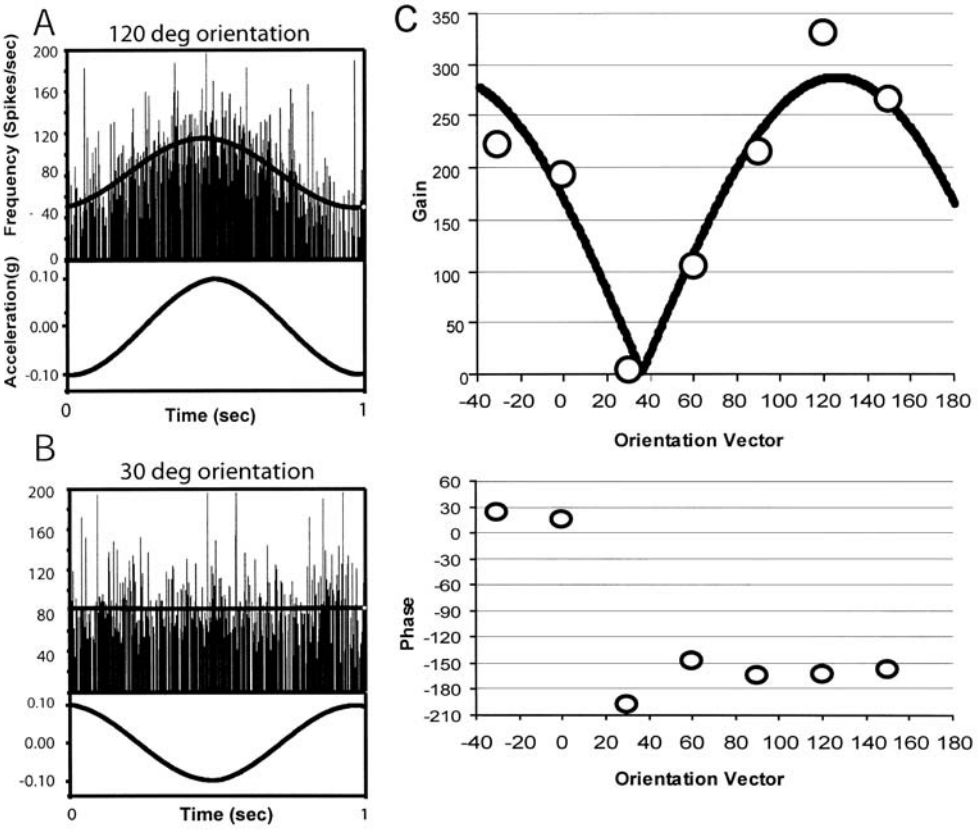

Fig. 1A–C Determination of maximum sensitivity vectors for utricular afferents. **A** The response of the afferent during translation with an orientation vector of 120°. This is the orientation that resulted in the greatest response of those orientations tested for this unit. The *upper panel* demonstrates the binned cycle histogram with the fitted response. The *lower panel* demonstrates the fitted response to the stimulus position. **B** The response to a 30° orientation vector stimulus. **C** The responses at 30° intervals between –30° and +150° are plotted vs. the orientation angle and fit using a rectified cosine function. In this example, the gmax was determined to be 288 spikes s^{-1} g^{-1} and the Smax is 125°

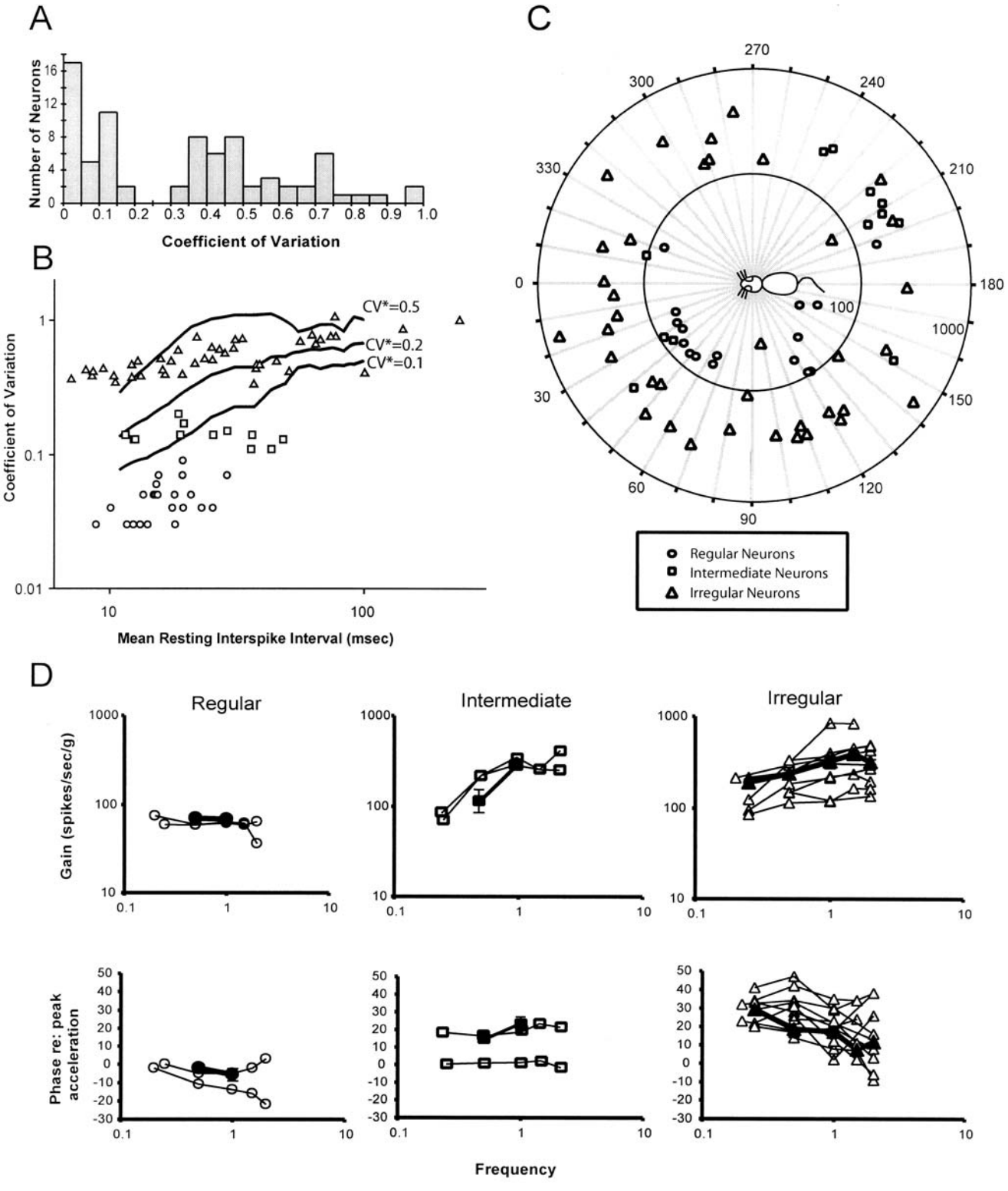

Fig. 2 **A** Distribution of CV of the physiologically characterized neurons. **B** CV vs. ISI (in milliseconds). *Circles* represent regular units (CV<0.1). Intermediate units ($0.1 \leq CV \leq 0.3$) are shown as *open squares* and irregular units (CV>0.3) as *open triangles*. The curves shown are based on the power-law regression formula $CV(ISI)=a(ISI)(CV^*)^{b(ISI)}$ (Goldberg et al. 1984) where the coefficients a(ISI) and b(ISI) are derived from chinchilla utricular afferents (Hullar and Minor 1999). Curves for CV*=0.1, 0.2, and 0.5 are shown. **C** Polar coordinate plots of gain (*r*) and maximum sensitivity vector (θ) for utricular afferents at stimulation frequencies of 0.5 Hz. The r axis is on log scale. The units recorded from the left vestibular nerve are reflected about the naso-occipital axis (0°–180°) such that all of the maximum sensitivity vectors are relative to the right ear. 0° is positive linear acceleration out of the animal's nose, 90° out of the left ear, and 270° out of the right ear. Note the preponderance of responses that are maximized out of the

position generating Smax was consistently offset by 90° from the head position generating the null response. A total of 65 units were recorded at 0.5 Hz with a gmax of 185±136 spikes s^{-1} g^{-1} (mean±SD; range of 23–648 spikes s^{-1} g^{-1}). A total of 32 units were recorded at 1.0 Hz with a gmax of 253±173 spikes s^{-1} g^{-1} (mean±SD; range of 45–848 spikes s^{-1} g^{-1}). Forty-eight percent of the units had a gmax greater than 200 spikes s^{-1} g^{-1} at 0.5 Hz compared to 63% of the units at 1.0 Hz.

The Smax and the associated gmax were plotted for all units characterized at 0.5 Hz stimulation (Fig. 2C). The Smax at 0.5 Hz for all units was scattered throughout the horizontal plane. The majority (43/65) of all units had Smax directed out the contralateral ear. Thirty-seven percent (24/65) of all units and 50% (8/16) of the regular firing units had Smax directed out the anterior, contralateral ear quadrant. The polar plot at 1.0 Hz (not shown) displays vectors of maximum sensitivity similar to the 0.5-Hz plot, except that the gains are higher for the intermediate and irregular units.

The responses of individual units to constant peak linear acceleration across multiple frequencies were obtained. Only two regular firing units were recorded at five frequencies. The gains of these neurons showed a flat frequency response (Fig. 2D). A total of 16 regular units were recorded at 0.5 and 9 at 1.0 Hz. These responses were consistent in demonstrating low gmax responses (69±28 and 68±18 spikes s^{-1} g^{-1}, mean±SD, respectively) throughout the tested range. The range of gmax for regular units at 0.5 Hz was from 30–155 spikes s^{-1} g^{-1}. The units recorded at 0.5 and 1.0 Hz showed an average phase lag of 2° at 0.5 Hz and 6° at 1.0 Hz (Fig. 2D).

There were two intermediate units recorded at five frequencies. These neurons showed a three to four-fold gain enhancement as stimulation frequency was increased (Fig. 2D). A total of 12 units recorded at 0.5 Hz (118±106 spikes s^{-1} g^{-1}, mean±SD, range 23–332) and 5 at 1.0 Hz (288±63 spikes s^{-1} g^{-1}, mean±SD, range 215–357) were consistent in demonstrating higher gmax at higher stimulation frequencies. The units recorded at 0.5 and 1.0 Hz showed an average phase lead of 16° at 0.5 Hz and 23° at 1.0 Hz (Fig. 2D).

There were ten irregular units characterized at four or more frequencies between 0.2 and 2.0 Hz. These units demonstrated the highest gains and showed a two to three-fold gmax enhancement as frequency increased (Fig. 2D). A total of 37 irregular units recorded at 0.5 Hz (256±127 spikes s^{-1} g^{-1}, mean±SD, range 39–648 spikes s^{-1} g^{-1}) and 18 at 1.0 Hz (324±166 spikes s^{-1} g^{-1}, mean±SD, range 118–848 spikes s^{-1} g^{-1}) were consistent in showing an increasing gmax at higher frequencies and a higher gmax than regular units. On average, the irregular units showed an average phase lead of 29° at 0.25 Hz decreasing to 12° at 2.0 Hz (Fig. 2D).

The variability of the response gains with the regularity of the unit was statistically significant at 1.0 and 0.5 Hz (ANOVA, $P<0.05$). At 0.5 Hz, the mean gmax of the irregular units were larger compared to that of the regular ($P<0.001$) and intermediate ($P<0.01$) units, though the mean gmax for the intermediate and regular units were not significantly different. At 1.0 Hz, the mean gmax of regular units was smaller compared to the intermediate ($P<0.001$) and irregular ($P<0.01$) units, but the gmax of intermediate and irregular units were not significantly different.

Measures of irregularity, particularly CV, vary with the firing rate of the afferent (Goldberg and Fernández 1971; Blanks et al. 1975). Correction for this variability can be attained by empirical formulas developed to relate the CV at the recorded ISI to a measure (CV*) that is a normalized CV adjusted to a standard mean interval of 15 ms (Goldberg et al. 1984). Development of the empirical formula requires a population of afferents studied at various head tilts to develop the relationship between CV and ISI. This was not done for the current data set. However, CV* values were developed using coefficients developed from recordings of utricular afferents in the chinchilla (Hullar and Minor 1999). Use of CV* developed from chinchilla data reclassified 12 afferents into more regular groups (Fig. 2B). For only one of these neurons was dynamic data collected at multiple frequencies, and use of CV* did not change any of the conclusions or statistical analyses presented above.

Discussion

Responses of utricular afferents to natural stimuli have been published in a number of species. Mammalian studies, with exception of one recent study (Angelaki and Dickman 2000), have used purely tilt motions (Fernández et al. 1972; Tomko et al. 1981; Dickman et al. 1991) or eccentric rotation (Fernández and Goldberg 1976a, b; Goldberg et al. 1990) to produce linear acceleration stimuli. The current study and others (Si et al. 1997; Angelaki and Dickman 2000) utilizing translational stimulation produce similar conclusions to the studies using other types of linear force stimuli.

Early reports in the monkey and later in the chinchilla emphasized the difference in responses of irregular and regular otolith units (Fernández and Goldberg 1976b; Goldberg et al. 1990). Unlike previous studies in monkeys and chinchillas (Goldberg et al. 1984; Baird et al. 1988; Goldberg et al. 1990; Hullar and Minor 1999), normalized CV was not used in the current experiments. While normalization provides a more absolute measure of regularity than CV, the necessary data to develop normalized CV for gerbil utricular afferents are not available. Use of coefficients developed in the chinchilla,

contralateral (*left*) ear. **D** Bode plots of frequency vs. gain for utricular afferents. *Open symbols* are individual units and *filled symbols* are averages for that frequency. *Circles* regular units, *Squares* intermediate units, *Triangles* irregular units, *Error bars* standard error of the mean. Many of the error bars are not seen because they approximate the size of the symbol. Phase is that which was found at the tested orientation closest to the calculated Smax

while reclassifying a number of afferents, did not change the conclusions from our analysis.

There was a clear relationship between discharge regularity and the dynamics of neuronal responses in gerbils. The most regularly firing neurons demonstrated flat gain responses, while irregularly firing neurons showed more phasic response dynamics. The magnitude of the high frequency gain enhancement was similar in gerbils to squirrel monkeys and chinchillas, though we tested a narrower band of frequencies. Similarly, the phase near zero for regular units and a modest phase lead for intermediate and irregular units is consistent with the response dynamics reported in those species (Fernández and Goldberg 1976b; Goldberg et al. 1990). The utricular afferents in gerbils do, however, show less of a phase lead in irregular units at higher frequencies.

Examination of the maximum sensitivity vectors of gerbil otolith afferent neurons demonstrated a greater preponderance of units responding to contralateral vectors of linear acceleration across the horizontal plane of the utricular macula. This is consistent with prior studies referenced to either position or linear acceleration in the monkey (Fernández and Goldberg 1976a; Angelaki and Dickman 2000), cat (Loe et al. 1973), and pigeon (Si et al. 1997) since linear acceleration out of the contralateral ear is equivalent to ipsilateral tilt stimulation. This expected similarity is likely due to the relatively asymmetric division of the utricular sensory neuroepithelium with a laterally located striola, resulting in a relatively larger amount of epithelium in the medial extra-striolar zone than in the lateral extra-striolar zone (Fernández and Goldberg 1976a; Si et al. 2003). The same arrangement is seen in the gerbil (Purcell and Perachio 2001). In chinchilla, with a relatively symmetric utricular epithelium, almost equal numbers of units were excited by ipsilateral and contralateral head tilts (Goldberg et al. 1990).

In summary, we have shown utricular afferent neurons in gerbils have response dynamics to translational stimulation that are similar to those described in other species. The gerbil, in our view, is an attractive model for analysis of the vestibular system. In previous studies, we have examined the central projections of the gerbil afferents, including those of the utricular nerve (Purcell and Perachio 2001; Newlands et al. 2002). The current data taken in conjunction with those morphological studies and other neurophysiological assessments of central vestibular neurons (Kaufman et al. 2000) will enable future examination of vestibular function in this species.

Acknowledgements Work was supported in part by the N.I.H. (DC 00385). We thank Drs. Tim Hullar and Lloyd Minor for use of their chinchilla utricular afferent coefficients for the development of CV*.

References

Angelaki DE, Dickman JD (2000) Spatiotemporal processing of linear acceleration: primary afferent and central vestibular neuron responses. J Neurophysiol 84:2113–2132

Angelaki DE, Bush GA, Perachio AA (1993) Two-dimensional spatiotemporal coding of linear acceleration in vestibular nuclei neurons. J Neurosci 13:1403–1417

Baird RA, Schuff NR (1994) Peripheral innervation patterns of vestibular nerve afferents in the bullfrog utriculus. J Comp Neurol 342:279–298

Baird RA, Desmadryl G, Fernández C, Goldberg JM (1988) The vestibular nerve of the chinchilla. II. Relation between afferent response properties and peripheral innervation patterns in the semicircular canals. J Neurophysiol 60:182–203

Blanks RH, Estes MS, Markham CH (1975) Physiologic characteristics of vestibular first-order canal neurons in the cat. II. Response to constant angular acceleration. J Neurophysiol 38:1250–1268

Curthoys IS, Betts GA, Burgess AM, MacDougall HG, Cartwright AD, Halmagyi GM (1999) The planes of the utricular and saccular maculae of the guinea pig. Ann New York Acad Sci 871:27–34

Dickman JD, Angelaki DE, Correia MJ (1991) Response properties of gerbil otolith afferents to small angle pitch and roll tilts. Brain Res 556:303–310

Fernández C, Goldberg JM (1976a) Physiology of peripheral neurons innervating otolith organs of the squirrel monkey. I. Response to static tilts and to long-duration centrifugal force. J Neurophysiol 39:970–984

Fernández C, Goldberg JM (1976b) Physiology of peripheral neurons innervating otolith organs of the squirrel monkey. III. Response dynamics. J Neurophysiol 39:996–1008

Fernández C, Goldberg JM, Abend WK (1972) Response to static tilts of peripheral neurons innervating the otolith organs of the squirrel monkey. J Neurophysiol 35:978–997

Fernández C, Goldberg JM, Baird RA (1990) The vestibular nerve of the chinchilla III. Peripheral innervation patterns in the utricular macula. J Neurophysiol 63:767–780

Goldberg JM, Fernández C (1971) Physiology of peripheral neurons innervating semicircular canals of the squirrel monkey. III. Variations among units in their discharge properties. J Neurophysiol 34:676–684

Goldberg JM, Smith CE, Fernández C (1984) Relation between discharge regularity and responses to externally applied galvanic currents in vestibular nerve afferents of the squirrel monkey. J Neurophysiol 51:1236–1256

Goldberg JM, Desmadryl G, Baird RA, Fernández C (1990) The vestibular nerve of the chinchilla IV. Discharge properties of utricular afferents. J Neurophysiol 63:781–790

Hullar TE, Minor LB (1999) High-frequency dynamics of regularly discharging canal afferents provide a linear signal for angular vestibuloocular reflexes. J Neurophysiol 82:2000–2005

Kaufman GD, Shinder ME, Perachio AA (2000) Convergent properties of vestibular-related brain stem neurons in the gerbil. J Neurophysiol 83:1958–1971

Lindeman HH (1969) Studies on the morphology of the sensory regions of the vestibular apparatus. Ergeb Anat Entwicklungsgesch 42:1–113

Loe PR, Tomko DL, Werner G (1973) The neural signal of angular head position in primary afferent vestibular nerve axons. J Physiol Lond 230:29–50

Newlands SD, Purcell IM, Kevetter GA, Perachio AA (2002) Central projections of the utricular nerve in the gerbil. J Comp Neurol 452:11–23

Perachio AA, Correia MJ (1983) Responses of semicircular canal and otolith afferents to small angle static head tilts in the gerbil. Brain Res 280:287–298

Purcell IM, Perachio AA (2001) Peripheral patterns of terminal innervation of vestibular primary afferent neurons projecting to the vestibulocerebellum in the gerbil. J Comp Neurol 432:48–61

Si X, Angelaki DE, Dickman JD (1997) Response properties of pigeon otolith afferents to linear acceleration. Exp Brain Res 117:242–250

Si X, Zakir MM, Dickman JD (2003) Afferent innervation of the utricular macula in pigeons. J Neurophysiol 89:1660–1677

Tomko DL, Peterka RJ, Schor RH (1981) Responses to head tilt in cat eighth nerve afferents. Brain Res 41:216–221